Theor Chem Acc (1999) 102:237–243
DOI 10.1007/s00214980m104

Theoretical
Chemistry Accounts

Regular article

Density functional study of ethylene oxidation on an Ag(111) surface*

Hisayoshi Kobayashi[1], **Katsumi Nakashiro**[2], **Tomoatsu Iwakuwa**[2]

[1] Department of Chemical Technology, Kurashiki University of Science and the Arts,
2640 Tsurajima, Nishinoura, Kurashiki 712-8505, Japan
[2] Mitsubishi Chemical Co., Yokkaichi Plant, 1 Toho-cho, Yokkaichi 510, Japan

Received: 2 July 1998 / Accepted: 9 September 1998 / Published online: 8 February 1999

Abstract. The mechanism of ethylene epoxidation on Ag surfaces has been investigated using the density functional method and Ag_n clusters ($n = 3$ to 10) modeling the Ag(111) surface. The adsorption energy of O_2 to the Ag clusters was strongly dependent on the HOMO level of the cluster, and the clusters with higher HOMO levels afforded larger O_2 adsorption energies. The energetics was investigated for both the molecular and atomic oxygen epoxidation mechanisms. For the atomic oxygen mechanism, epoxidation was found to proceed without an activation energy, whereas a small amount of activation energy (about 5 kcal/mol) was calculated for the molecular oxygen mechanism.

Key words: Density functional method – Ethylene epoxidation – Ag clusters

1 Introduction

There is a long history of research on ethylene oxide (epoxide) formation. Ag is the only element which catalyzes epoxide formation. Epoxidation has been one of the most important industrial processes, and the development of epoxidation catalysts is still continuing intensively and has been one of the subjects of basic research [1–4]. Several theoretical approaches have been presented: the extended Hückel [5], LCAO-Xα [6], Hartree-Fock (HF) + MP 3 [7], GVB-CI [8], and the density functional (DF) method [9]. Carter and Goddard [8] suggested a surface atomic oxyradical as the active oxygen species. McKee [7] supported the molecular oxygen mechanism but Hoek et al. [9] supported the atomic oxygen mechanism suggested by Carter and Goddard; however, these authors [7, 9] were mainly concerned with the role of subsurface promoters, and the energetics of the reaction was not investigated.

Recently, Nakatsuji and coworkers studied the energetics of the molecular and atomic oxygen mechanisms in detail using the HF + MP2 [10] and the SAC-CI method [11–12]. They concluded that epoxidation is selectively preferable for the molecular oxygen mechanism, whereas epoxidation and complete oxidation compete in the atomic oxygen mechanism. They used a Ag dimer and their dipped adcluster model. In their scheme, they compared the total energies among the systems with the different number of electrons along the reactions.

Thanks to recent progress in DF methods, it is known that the DF method is especially suitable for systems including several heavy atoms and the systems the electron correlation is important. In this article we present further aspects of the energetics and the structural changes of the reaction mechanisms using the recent version of DF methods and more realistic (i.e., larger) cluster models, in which enough electron density is expected to be donated to the adsorbing oxygen species. The energy is discussed using the systems with a constant number of electrons, i.e., only the neutral clusters.

2 Method of calculation and models

The hybrid HF and DF method is used in this work [13, 14]. This method is implemented in the Gaussian 94 program [15]. The parametrization suggested by Gill et al. [14] is used, i.e., 0.2, 0.8, and 0.72 for the HF, Slater [16], and Becke exchange functionals [17] and 0.19 and 0.81 for the Vosko-Wilk-Nusair [18] and Lee-Yang-Parr correlation functionals [19]. The Los Alamos effective core potential is used for the Ag atom [20] to replace the Kr core. The corresponding valence basis set is (3*s*3*p*4*d*)/[2*s*2*p*2*d*]. For C, O, and H atoms, the Dunning-Huzinaga full double zeta (D95) basis set is used [21]: (10*s*5*p*)/[3*s*2*p*] and (4*s*)/[2*s*], respectively. For the energetics of epoxidation, after the structures of local minima and the transition states (TSs) are optimized, these energies are reevaluated with a larger basis set, in which the diffuse *s* and *p* functions of $\alpha = 0.059$ and the polarization *d* functions of $\alpha = 2.704$ and 0.535 are added on the O atoms, according to the work of Nakatsuji et al. [10].

*Contribution to the Kenichi Fukui Memorial Issue

Correspondence to: H. Kobayashi

Different researchers used different Ag clusters in their studies. First we examined how the adsorption energy depends on the size and shape of the clusters used. The O_2 molecule was adsorbed to nine Ag clusters, as shown in Fig. 1. The clusters are labeled Ag_3(linear), Ag_3(triangular), Ag_4(tetrahedral), Ag_4(lozenge), Ag_5, Ag_6, Ag_7, Ag_8, and Ag_{10}. As we will mention later, two conditions are necessary for clusters to simulate epoxidation. (1) A relatively high energy for the cluster HOMO level, and (2) a lozenge (diamond)-shaped area for coadsorption of O_2 and C_2H_4. The Ag_5 cluster is the smallest one satisfying these conditions, and we employed this cluster intensively for elucidation of the epoxidation mechanism.

Throughout this work, the structure of the Ag clusters is fixed, and the structure and relative orientation of C_2H_4 and O_2 with respect to the cluster is optimized. The stabilization energy is defined as $\Delta E = [E(\text{Ag cluster}) + E(C_2H_4) + xE(O_2)] - E(\text{combined system})$, where $x = 1$ or $1/2$ depending on molecular or atomic oxygen. ΔE is positive for stable adsorption.

3 Results and discussion

3.1 Adsorption of O_2 molecules on Ag clusters

O_2 molecule adsorption is examined with 13 configurations on nine clusters. The spin multiplicity for the ground state is shown in Table 1. For almost all Ag_n clusters, the ground state is that of the lowest spin multiplicity, i.e., the singlet for even n and the doublet for odd n. Two exceptions are the Ag_4(tetrahedral) and the Ag_{10} clusters, for which the triplet state is the ground state. For Ag_nO_2 systems, the lowest spin state is the ground state again except for the Ag_6O_2 and Ag_8O_2 systems, for which the triplet state is the ground state. It is reasonable that for the systems with weak O_2-Ag_n interactions, the O_2 moiety prefers the triplet state. The HOMO levels of free clusters and the O_2 adsorption energies are shown in Table 1. There seems to be a correlation between them: the clusters with higher HOMO levels afford larger adsorption energies. This trend is reasonable since O_2 adsorption is known to require large electron drift into the O_2 moiety. If we say tentatively that a stabilization energy of more than 20 kcal/mol is an indication of strong adsorption, the borderline in the HOMO level is −3.8 eV. Among the nine clusters, strong adsorption occurs for the Ag_3(triangular), Ag_4(tetrahedral), Ag_5, and Ag_7 clusters. Ag_6 and Ag_8 clusters have very small adsorption energies due to their deep HOMO levels.

Ag_{10} and probably Ag_4(tetrahedral) clusters deviate from this trend. In their case, the free cluster and the O_2 molecule are triplet states, but the combined systems are singlet states. Tentatively, if we take the HOMO level and the total energy for the singlet state (not the ground state) of these Ag clusters, it is more favorable for this trend.

The HOMO level of the cluster used is higher than the work function of the Ag(111) surface reported as 4.74 eV [22]. Although we used the cluster modeling the (111) surface, we think the reaction occurs at some localized structures such as adatoms or terraces on polycrystalline catalysts, and the "effective" work function is thought to be higher than the monocrystalline value. Second, we admit that the present models overestimate the electron donating character. It is well known that in industrial catalysts, promoters are necessary for epoxidation reactions, and pure Ag surfaces are not active enough. We do not deal with the promoters in this work, but the small clusters implicitly reflect the effects of electron donating promoters.

Figure 1 shows the optimized configurations of Ag_nO_2 systems. For the Ag_3 to Ag_5 clusters, adsorption is examined in different O_2 configurations. The asymmetrical configuration is the local minimum rather than the symmetrical T-shaped one for the Ag_3 linear cluster. For the Ag_3 triangular cluster, the edge configuration is more stable than the plane one, but the former is not acceptable as the adsorption model. On the contrary, the plane configuration is more stable than the edge one for the Ag_4 tetrahedral cluster. For the Ag_4(lozenge) and Ag_5 clusters, the parallel configuration, where the O—O axis is parallel to the Ag—Ag axis, and the perpendicular configuration, where their projection crosses at right angles, are compared with each other. The former has the larger stabilization energy in both models. For the Ag_4(lozenge-parallel)O_2 configuration, the O—O bond is stretched to 1.58 Å. The elongation of the O—O bond is well correlated with the amount of negative charge on the O_2 moiety. In this system, O_2 possesses the maximum value of −0.84 e.

Among the four clusters with the larger adsorption energies, we employed the Ag_5 cluster to investigate epoxidation. We adopted the orientation of the coadsorption system shown in Fig. 2, following the work of Nakatsuji et al. [10]. For the coadsorption and successive reactions, the lozenge-shaped area is necessary to simulate the reaction within the cluster. The Ag_4(lozenge) and the larger clusters have this stage. However, the small O_2 adsorption energy indicates that the Ag_4(lozenge) cluster is not adequate, and the Ag_5 cluster is adopted. In the following, all the calculations are carried out with the doublet state, which is confirmed to be the ground state.

3.2 Adsorbed structures of C_2H_4 and O_2 molecules on the Ag_5 cluster

The Ag_5 cluster consists of the lozenge-shape four-atom facet and one second layer atom. This cluster has the symmetry plane perpendicular to the "surface", and adsorption and epoxidation are assumed to conserve this symmetry. The optimized structure for the adsorbed O_2 molecule is shown in Fig. 1. The parallel configuration of the O_2 molecule on the Ag_5 cluster is more stable than the perpendicular one by 6 kcal/mol. However, the latter is clearly adequate for interaction with C_2H_4, and we adopted this configuration. The O—O bond length, R_{O-O} is calculated to be 1.42 Å and elongated by 0.15 Å compared to the free molecule. Both the O atoms have a same negative charge of −0.29.

The optimized structure for the coadsorbed state is shown in Fig. 2. R_{O-O}, R_{C-C}, and R_{O-C} are calculated to be 1.55, 1.51, and 1.51 Å, respectively. R_{C-C} is stretched by 0.16 Å compared to free C_2H_4. The negative charges on the O atom increase to −0.42 and −0.35. The charges of the two methylene groups (i.e., the charge summed over the C atom and the two connecting H

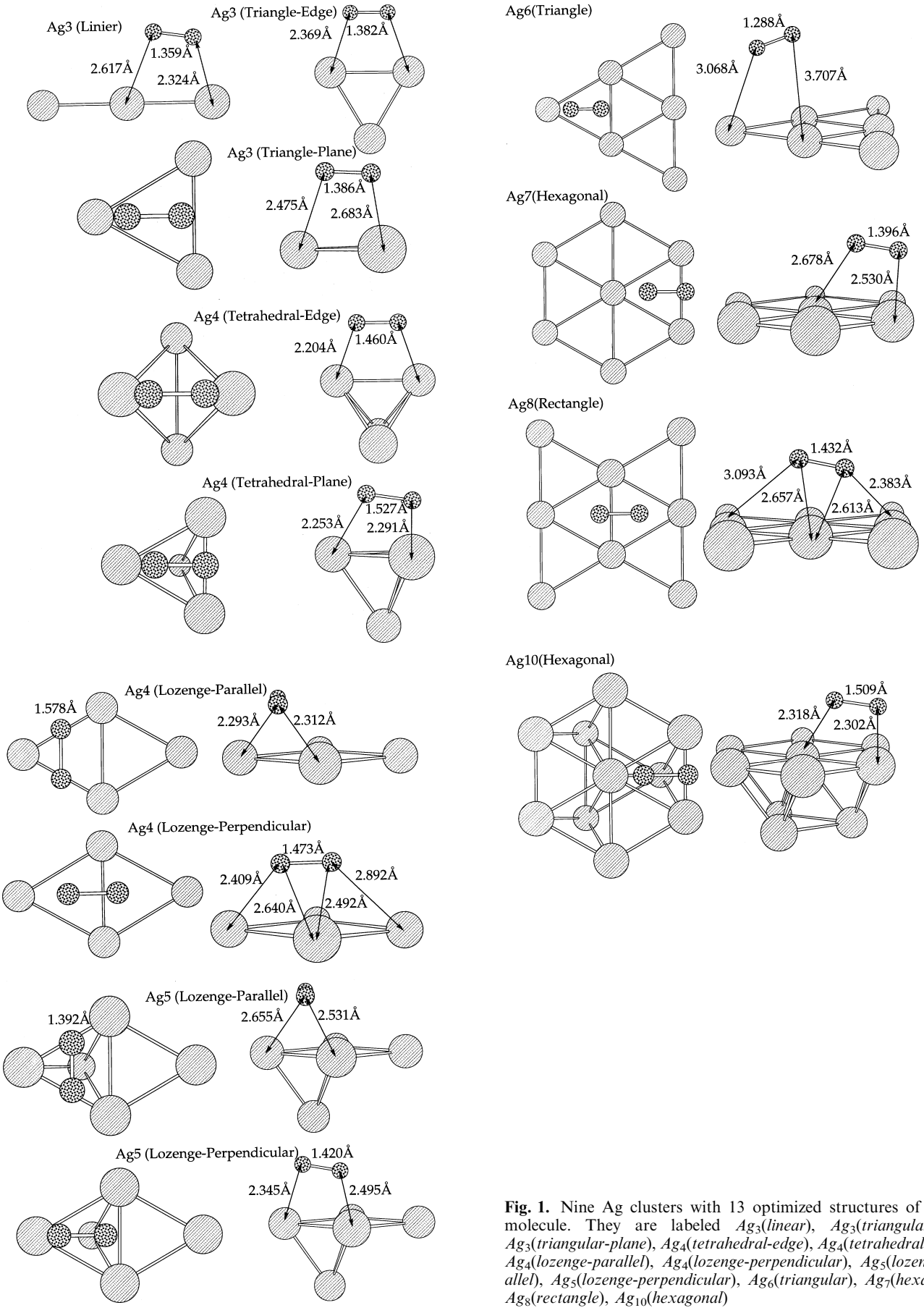

Fig. 1. Nine Ag clusters with 13 optimized structures of the O_2 molecule. They are labeled Ag_3(*linear*), Ag_3(*triangular-edge*), Ag_3(*triangular-plane*), Ag_4(*tetrahedral-edge*), Ag_4(*tetrahedral-plane*), Ag_4(*lozenge-parallel*), Ag_4(*lozenge-perpendicular*), Ag_5(*lozenge-parallel*), Ag_5(*lozenge-perpendicular*), Ag_6(*triangular*), Ag_7(*hexagonal*), Ag_8(*rectangle*), Ag_{10}(*hexagonal*)

Table 1. Spin multiplicity of Ag_n and Ag_nO_2 systems, HOMO level for Ag_n clusters, and adsorption energy with an O_2 molecule

	Multiplicity[a]	E (HOMO) (eV)	ΔE (kcal/mol)[b]
Ag_3 (linear)	2, 2	−4.46	9.2
Ag_3 (triangular-edge)	2, 2	−3.37	40.4
Ag_3 (triangular-plane)	2, 2		27.0
Ag_4 (tetrahedral-edge)	3, 1	−3.73 (−3.35)[c]	20.9 (30.7)[d]
Ag_4 (tetrahedral-plane)	3, 1		39.2 (49.0)[d]
Ag_4 (lozenge-parallel)	1, 1	−4.03	5.3
Ag_4 (lozenge-perpendicular)	1, 1		3.8
Ag_5 (lozenge-parallel)	2, 2	−3.62	33.8
Ag_5 (lozenge-perpendicular)	2, 2		28.0
Ag_6 (triangular)	1, 3	−4.71	2.8
Ag_7 (hexagonal)	2, 2	−3.27	25.4
Ag_8 (rectangular)	1, 3	−3.89	5.0
Ag_{10} (hexagonal)	3, 1	−3.62 (−3.36)[c]	13.3 (19.5)[d]

[a] The first and second digits represent the spin multiplicity for the Ag_n and the Ag_nO_2 systems, respectively
[b] Positive value means stabilization
[c] The value in parentheses is the HOMO level for the singlet state of the Ag_n cluster
[d] The value in parentheses is the adsorption energy relative to the total energy in the singlet state of the Ag_n cluster

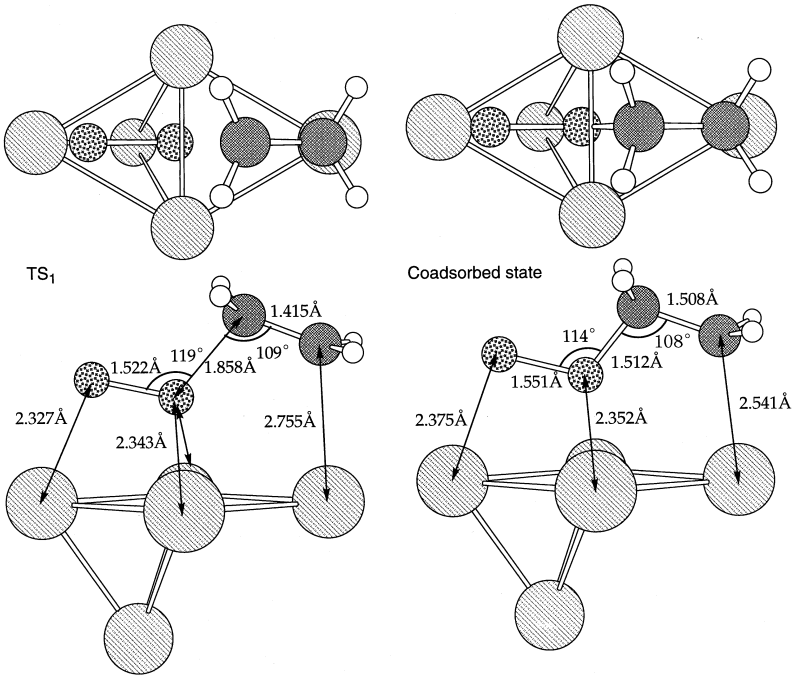

Fig. 2. Optimized structures of TS_1 and the $O_2 + C_2H_4$ coadsorbed state for the molecular oxygen mechanism. TS_1 is located between the O_2 adsorption and coadsorbed states

atoms) are +0.22 (adjacent to O) and −0.23 (terminal). Thus, the polarization is enhanced within the C_2H_4 molecule, whereas the net charge on C_2H_4 is very small. The unpaired spin is distributed over the two O atoms before C_2H_4 adsorption, but delocalized on the terminal C atom and two terminal Ag atoms after adsorption.

The coadsorption of C_2H_4 is an activating process, and this local minimum is surrounded by the two TSs: TS_1 for the O_2 adsorption side and TS_2 for the product side, and they are shown in Figs. 2 and 3, respectively. The structural changes from TS_1 to the coadsorbed state are a decrease in the O—C distance and an elongation of the C—C bond. From the coadsorbed state to TS_2, the O—O distance increases from 1.51 to 1.86 Å. The other internal parameters characterizing the $O_2C_2H_4$ zigzag structure are almost unchanged from TS_1 to TS_2. The product consists of epoxide adsorbed to the terminal Ag atom and an atomic O adsorbed at the three fold-site, as shown in Fig. 3. Among the coadsorbed state, TS_2, and the product, the C—C and C—O bond lengths are hardly changed.

The energy profiles of epoxidation are shown in Fig. 4. For the molecular oxygen mechanism, adsorption of an O_2 molecule stabilizes the system by 16 kcal/mol. The activation energies for the two TSs are 2 and 5 kcal/mol above the zero-energy level, respectively, and the barrier heights measured from the O_2 adsorption state are 17 and 21 kcal/mol, respectively. The local minimum of the coadsorbed state is located 11 kcal/mol above the O_2 adsorption state. After TS_2, the adsorption energy increases by 39 kcal/mol. This large stabilization is ascribed to epoxide formation and an atomic oxygen

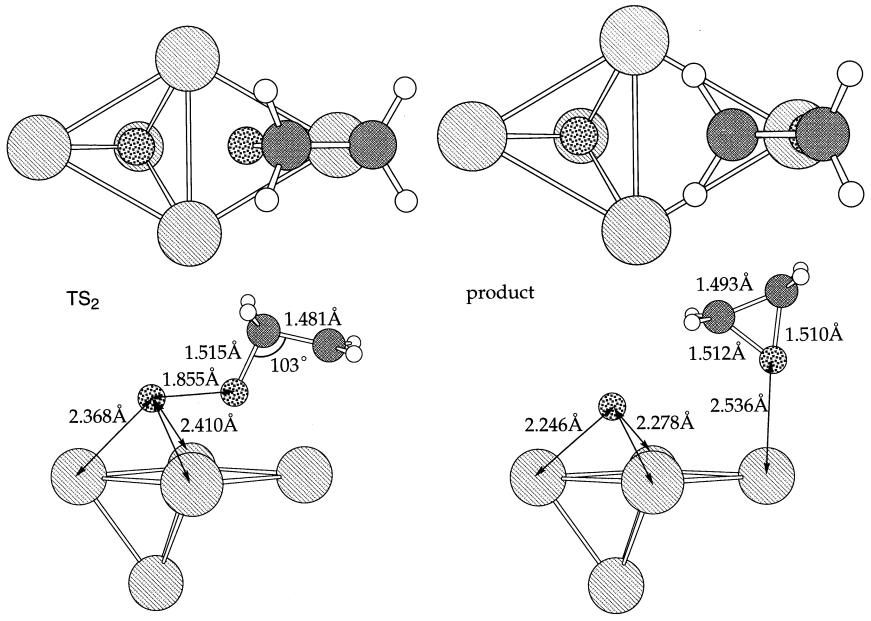

Fig. 3. Optimized structures of TS_2 and the product for the molecular oxygen mechanism. TS_2 is located between the coadsorbed state and the product. The product consists of adsorbed epoxide and adsorbed atomic oxygen

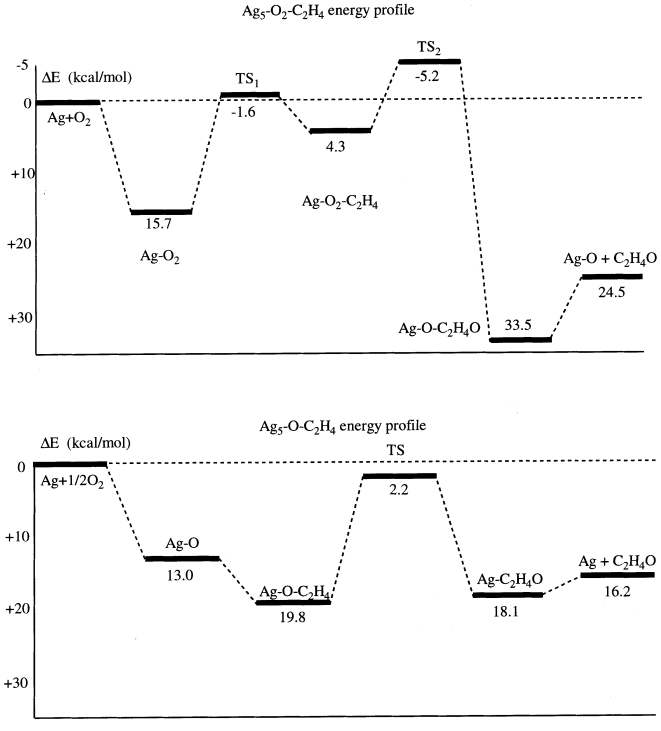

Fig. 4. Energy profiles for molecular (*top*) and atomic (*bottom*) oxygen epoxidation mechanisms

adsorbed at the three-fold site. The desorption energy of the epoxide is calculated to be 9 kcal/mol.

3.3 Adsorbed structures of C_2H_4 and O atoms on an Ag_5 cluster

Optimized structures for the adsorbed O atom and the coadsorbed C_2H_4 are shown in Fig. 5. The O atom is stabilized at the center of the three-fold site. This structure is the same as that produced as the product of the molecular oxygen mechanism. The O atom is highly charged, −0.62, and it is larger than the charge summed over the adsorbed O_2 molecule. The charge of C_2H_4 is positive, and C_2H_4 donates 0.13e to the O atom. These results suggest that the adsorbed atomic oxygen requires more negative charge than the molecular oxygen. In the coadsorbed state, the O atom closely binds to C_2H_4, $R_{O-C} = 1.48$ Å, whereas the elongation of the C—C bond is smaller than in the case of molecular oxygen. The unpaired spin is divided between the O atom and the most distant Ag atom, but is solely localized on the terminal C atom after C_2H_4 adsorption.

Structures for the TS and the epoxide are shown in Fig. 6. Comparing the structures with those for the molecular oxygen mechanism, the TS structure is closer to the product, i.e., the so-called late TS. The C—C—O angle is 75°, whereas it is 103° in TS_2 for the molecular oxygen case. (In the epoxide it is almost 60°.) In both the coadsorbed states, the C—C—O angles have similar values: 111° for Ag—O—C_2H_4 and 108° for Ag—O_2—C_2H_4. In the course of the coadsorbed state, TS (or TS_2) and the product, the C—O and C—C bond lengths are more changeable than in the molecular oxygen mechanism. R_{O-C} is increases from 1.48 to 1.51 Å. It is common to both mechanisms that R_{C-C} is shortest for the TS (or TS_2).

The energy profile is shown in Fig. 4. The adsorption of C_2H_4 onto the surface O atom is an exothermic process, and the adsorption energy increases by 7 kcal/mol. The barrier height measured from the coadsorbed state is 18 kcal/mol, and this energy is 2 kcal/mol below the zero-energy level. After the TS, the adsorbed epoxide is formed, and the stabilization is relatively small (16 kcal/mol). This result is in contrast to the molecular oxygen mechanism, but reasonable since no more oxygen species exist on the surface. The desorption energy of the epoxide is only 2 kcal/mol.

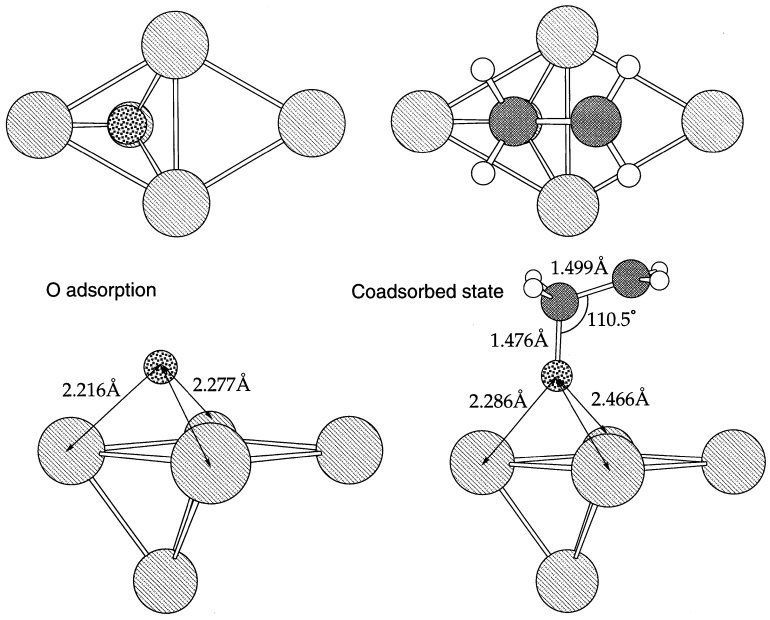

Fig. 5. Optimized structures of O adsorption and the O + C_2H_4 coadsorbed state for the atomic oxygen mechanism

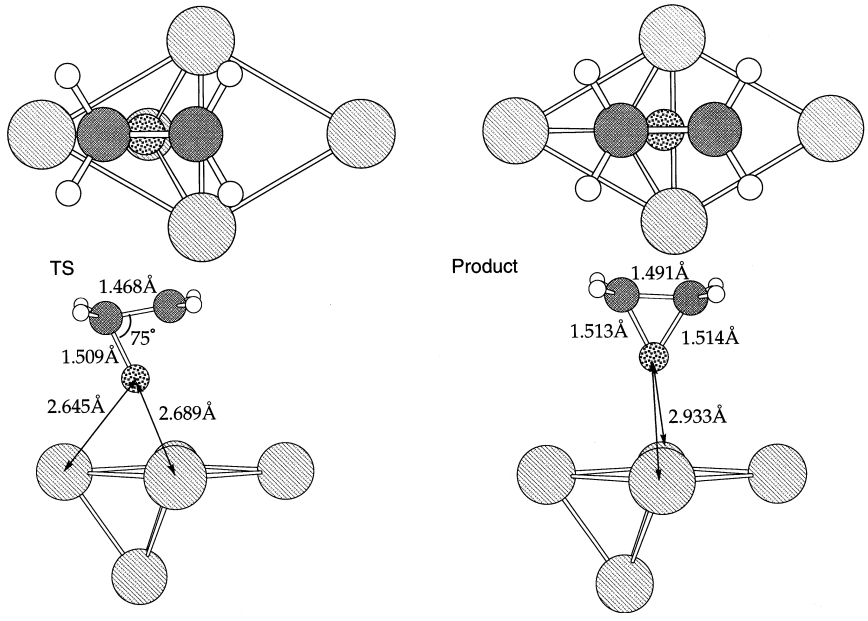

Fig. 6. Optimized structures of the TS and the product for the atomic oxygen mechanism. The product is adsorbed epoxide

Comparing both mechanisms, it is said that for the molecular oxygen mechanism, TS_2 is close to the coadsorbed state (early TS) with respect to the energy (Fig. 4) and the geometry (Figs. 2, 3). On the other hand, for the atomic oxygen mechanism, TS is close to the product (late TS) with respect to the energy (Fig. 4) and the geometry (Figs. 5, 6). Judging from the activation energy, the atomic oxygen mechanism seems to be more favorable. However, the barrier height for the molecular mechanism is 5 kcal/mol at most and so the molecular oxygen mechanism is not completely eliminated.

4 Concluding remarks

In this work, the mechanism of epoxide formation is investigated using the hybrid DF method, and the Ag_5 cluster model. The calculation shows that the atomic oxygen mechanism has a smoother reaction path without an activation energy. On the other hand, an activation energy of 5 kcal/mol is calculated for the molecular oxygen mechanism. Since the activation energy is not so large, this reaction seems to occur under usual reaction conditions above room temperature. Irrespective of the molecular oxygen mechanism, our calculation showed that epoxidation could proceed through the atomic oxygen mechanism. A selectivity higher than sixth-sevenths is possible if side reactions are suppressed effectively.

Acknowledgement. This work was supported by the grants from the Ministry of Education, Science and Culture of Japan (Nos. 09218257 and 09650865).

Appendix

The TSs are searched for in the following way. The C—C—O angle is adopted as the approximate reaction coordinate in the neighborhood of the TS. The restricted optimization for the other internal parameters is carried out stepwise. From the point with the highest energy, the TS search is started without restriction. More practically, the analytical second derivatives are evaluated once using the different all-electron basis set, and then reused for the MCP calculations.

Effects of the polarization *d* functions on O atoms are remarkable. The *s* and *p* diffuse functions lower the total energy of O_2 by only 4.6 kcal/mol, whereas further augmentation by the two *d* functions lowers the total energy by 29.1 kcal/mol. Interestingly this energy lowering is larger for $\mathbf{O_2}$ and C_2H_4O than for the adsorption intermediates including Ag—O bonding, and this leads to a decrease in adsorption energy and an increase in activation energy.

References

1. Spencer ND, Lambert RM (1981) Chem Phys Lett 83: 388
2. Grant RB, Lambert RM (1985) J Catal 93: 92
3. Campbell CT (1985) J Phys Chem 89: 5789
4. Tan SA, Grant RB, Lambert RM (1987) J Catal 106: 54
5. Jørgensen KA, Hoffmann R (1990) J Phys Chem 94: 3046
6. Selmani A, Andzelm J, Salahub DR (1986) Int J Quantum Chem 29: 829
7. McKee ML, (1987) J Chem Phys 87: 3143
8. (a) Carter EA, Goddard WA III (1988) J Catal 112: 80; (b) Carter EA, Goddard WA III (1989) Surf Sci 209: 243
9. van den Hoek PJ, Baerends EJ, van Santen RA, (1989) J Phys Chem 93: 6469
10. Nakatsuji H, Nakai H, Ikeda K, Yamamoto Y (1997) Surf Sci 384: 315
11. Nakatsuji H, Hu Z, Nakai H, Ikeda K (1997) Surf Sci 387: 328
12. Nakatsuji H, Hu Z, Nakai H (1997) Int J Quantum Chem 65: 839
13. Becke AD (1993) J Chem Phys 98: 1372
14. Gill PMW, Johnson BG, Pople JA (1992) Int J Quantum Chem Symp 26: 319
15. Frisch MJ, Trucks GW, Schlegel HB, Gill PMW, Johnson BG, Robb MA, Cheeseman JR, Keith T, Petersson GA, Montgomery JA, Raghavachari K, Al-Laham MA, Zakrzewski VG, Ortiz JV, Foresman JB, Peng CY, Ayala PY, Chen W, Wong MW, Andres JL, Replogle ES, Gomperts R, Martin RL, Fox DJ, Binkley JS, Defrees DJ, Baker J, Stewart JP, Head-Gordon M, Gonzalez C, Pople JA (1995) Gaussian 94, revision B.3. Gaussian, Pittsburgh, Pa
16. Slater JC, (1951) Phys Rev 81: 385
17. Becke AD (1988) Phys Rev A 38: 3098
18. (a) Vosko SH, Wilk L, Nusair M (1980) Can J Phys 58: 1200l; (b) Wilk L, Vosko SH (1982) J Phys C 15: 2139
19. Lee C, Yang W, Parr RG (1988) Phys Rev B 37: 785
20. (a) Hay PJ, Wadt WR (1985) J Chem Phys 82: 270; (b) Wadt WR, Hay PJ (1985) J Chem Phys 82: 284; (c) Hay PJ, Wadt WR (1985) J Chem Phys 82: 299
21. Dunning TH Jr, Hay PJ (1976) In: Schaefer HF III (ed) Modern theoretical chemistry Plenum, New York, pl
22. Weast RC (ed) (1985) CRC handbook of chemistry and physics, 66th edn. CRC Press, Boca Raton, p.E-86